

Green synthesis and characterization of soluble starch-stabilized silver nanoparticles with evaluation of antioxidant, wound healing and anticancer activity

Oshin M Manchu^{1*}, Dr. S. Jasmin Sugantha Malar²

¹*Research Scholar, Reg: No: 22213282032005, Department of Chemistry and Research Centre, Women's Christian College, Nagercoil - 629001. Affiliated to Manonmaniam Sundaranar University, Abishekappatti, Tirunelveli - 627012, Tamil Nadu, India. E-mail: oshinmanchu2000@gmail.com

²Associate Professor & Research Supervisor, Department of Chemistry and Research Centre, Women's Christian College, Nagercoil -629001. Affiliated to Manonmaniam Sundaranar University, Abishekappatti, Tirunelveli - 627012, Tamil Nadu, India. E-mail: lovelinjasmin@gmail.com

Abstract

Soluble starch was used as a green reducing and stabilizing agent to synthesize the silver nanoparticles (SS-AgNPs) using an eco-friendly approach. The formation of AgNPs was confirmed by a distinct surface plasmon resonance peak observed at 432 nm in the UV-visible spectroscopy. Structural characterizations using X-ray Diffraction (XRD) showed sharp reflections corresponding to the face-centered cubic structure of silver, as well as crystallite sizes ranging from 14.72 to 17.60 nm, with an average of 15.83 nm. TEM analysis of nanoparticles showed predominantly spherical particles with an average size of 25.26 nm. SEM image revealed that the morphology was somewhat uniform with very little aggregation. It also confirmed elemental purity of the nanoparticles with strong silver signals by EDS. SS-AgNPs were synthesized and displayed low-to-moderate antioxidant capacity with a DPPH IC₅₀ of 303.45 µg/mL. Biocompatibility studies with HaCaT keratinocytes confirmed increased cell proliferation (~187% viability), making it an appropriate candidate for cell proliferation-based wound healing potential. The anticancer activity of MCF-7 breast cancer cells was observed to be strong with an IC₅₀ of 14.69 µg/mL, with apoptotic morphological alterations as well. Together, the results demonstrate that soluble starch can efficiently synthesize solid, crystalline silver nanoparticles with antioxidant, anticancer, and wound-healing activities.

Keywords: soluble starch, silver nanoparticles, biopolymers, antioxidant, anticancer activity, wound healing

Introduction

Nanotechnology is a rapidly growing area within materials science, chemistry, biology, and medicine. Silver nanoparticles (AgNPs), as one of the large family of nanomaterials, have received widespread interest on account of peculiar optical, catalytic, electrical, and biological properties [1]. They have nanoscale sizes and a much larger surface area to volume ratio, which gives them improved reactivity and multifunctional properties, which is applied in biomedical, pharmaceutical, agro-chemical, and environmental spheres [2]. AgNPs are typically prepared with powerful chemical reducing agents such as sodium borohydride (NaBH₄) or hydrazine which leads to toxicity, environmental effects, and limited biocompatibility. To address these limitations, biopolymer-assisted and green synthetic methods have emerged as very attractive pathways and strategies [3]. Soluble starch, an organic polysaccharide composed of amylose and amylopectin, can serve as an effective reducing and stabilizing agent for nanoparticle synthesis. Its rich hydroxyl groups can be used to reduce Ag⁺ to Ag⁰ (silver), and the metal structure can stabilize the nanoparticles via steric immobilization [4]. Starch is biodegradable, nontoxic, renewable, cheap, and readily available, which is favorable to the green synthesis of AgNPs. Due to the cohesive nature of the molecular architecture of starch, the same nucleation and nanoparticle growth can be achieved without large variability, which can lead to better stability, and the size of the particles can be adjusted [5]. Therefore, soluble starch-silver nanoparticles (SS-AgNPs) are a sustainable, biocompatible, and promising microencapsulative nanomaterial in the context of medical technology [6]. Extensive physicochemical characterization is required to characterize the biochemistry, shape, crystallinity, and elemental composition of the SS-AgNPs. UV-visible spectroscopy can be used to first confirm the synthesis of the nanoparticles. The characteristic surface plasmon resonance (SPR) band of metallic silver can be identified and discussed in parallel. X-ray Diffraction (XRD) is used for crystallinity, phase purity and average crystal size, with confirmation obtained for FCC silver. SEM shows the surface morphology and pattern of particle aggregates, while EDS detects elemental composition and purity. Transmission Electron Microscopy (TEM) allows visualization from a high position of nanoparticle size, shape, and lattice features, thus yielding valuable insight into overall structure homogeneity.

Together with the above characterization techniques, the physicochemical properties of the soluble starch-AgNPs are extensively characterized. The soluble starch-AgNPs possess not only characteristic properties of structure, but also biological functions that are beneficial for the development of therapeutic compounds. Silver nanoparticles act as antioxidants able to remove reactive oxygen species (ROS) and suppress oxidative stress-induced cell damage [7]. They are capable of inducing apoptosis and generating ROS in cancer cells at lower levels, whereas normal cells are spared owing to several mechanisms (ROS generation, mitochondrial disruption, DNA damage, apoptosis induction, etc.) [8][9]. AgNPs possess remarkable wound healing activity supported by their antimicrobial activity, potential on keratinocyte and fibroblast proliferation, enhancement of collagen deposition, and promotion of re-epithelialization [10]. The integration of a naturally occurring polymer, specifically soluble starch, can effectively increase AgNP cytocompatibility and stability and render them ideal candidates for skin regeneration, and for applications in clinical formulations [11]. With these benefits, the current investigation concentrates on the preparation of soluble starch-silver nanoparticles by using a green and sustainable method, and by thorough characterization using UV-visible spectroscopy, XRD, SEM, EDS, and TEM. The biological activity of the synthetic nanoparticles was studied in antioxidant studies, anticancer activity, and in vitro wound restoration studies. This comprehensive study provides scientific evidence for the potential application of Soluble starch-AgNPs in biomedicine and contributes to the development of safe, effective, and green nanoparticle-based therapeutic agents.

Materials and Methods

Soluble starch (analytical grade) was purchased from Nice Chemicals Pvt. Ltd., India. Silver nitrate (AgNO_3 , $\geq 99\%$ purity) was purchased from Molychem, India. All reagents were used without further purification. Deionized water was used throughout the study. All glassware used in the experiments was thoroughly cleaned and rinsed with deionized water prior to use to avoid contamination.

Soluble starch-silver nanoparticles (SS-AgNPs) synthesis

Silver nanoparticles were prepared by treating with soluble starch as reducing solution and stabilizing agent. Soluble starch solution was prepared by dissolving 1 g of soluble starch in 150 mL of deionized water. 1.7 g of AgNO_3 was dissolved into 200ml deionized water. From that silver nitrate solution 50 ml was taken and add up with soluble Starch solution. The reaction mixture was taken in a 250 ml beaker and heated on a magnetic stirrer with stirring at 70 °C for about 6 h. The formation of the soluble Starch silver nanoparticles was indicated by the colour change of the solution from white to brown. The synthesized soluble starch silver nanoparticles were dried and kept in an airtight container for further analysis.

Results and Discussion

UV-visible spectral analysis

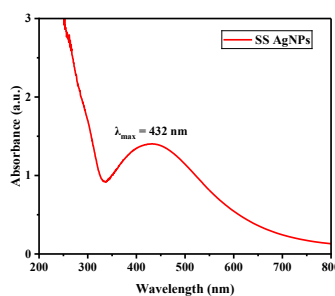


Figure 1. UV-visible spectrum of SS-AgNPs showing an SPR peak at 432 nm

The UV-visible absorption spectrum of SS-AgNPs were observed using a Shimadzu UV-1800 spectrophotometer in the range 200-800 nm. The formation of AgNPs was confirmed by a distinct surface plasmon resonance (SPR) band at 432 nm is shown (Figure:1). SPR is generated through the oscillation of the surface electrons in response to the excitation of light. Absence of secondary SPR peaks indicates limited aggregation of nanoparticles [12][13].

X-ray Diffraction (XRD) analysis

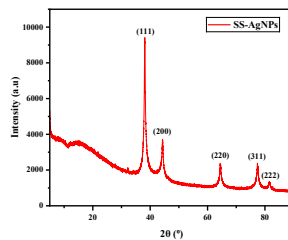


Figure 2. X-ray diffraction spectrum of SS-AgNPs

Table 1. Calculation of particle size of SS-AgNPs

Peak	2θ (°)	d-spacing (Å)	FWHM (°)	FWHM (rad)	θ (°)	θ (rad)	D (nm)
(111)	38.0915	2.36053	0.4774	0.008332	19.0458	0.3324	17.60
(200)	44.2800	2.04393	0.5584	0.009746	22.1400	0.3864	15.36
(220)	64.4312	1.44492	0.6379	0.011133	32.2156	0.5622	14.72
(311)	77.3891	1.23214	0.6170	0.010769	38.6946	0.6755	16.50
(222)	81.4964	1.18010	0.7012	0.012238	40.7482	0.7113	14.95
Average							15.83

The soluble starch-stabilized silver nanoparticles (SS-AgNPs) have been analyzed via XRD in normal scan mode by Bruker D8 ADVANCE diffractometer over a 2θ range of 5°-90° at a scan rate of 6°/min. These diffraction peaks at 38.09°, 44.28°, 64.43°, 77.39° and 81.49° correspond to the (111), (200), (220), (311) and (222) planes of face-centered cubic (FCC) silver. The calculated crystallite sizes from the five peaks based on the Debye-Scherrer equation were between 14.7-17.6 nm and an average crystallite size (D) of 15.83 nm. The observed XRD peaks correspond to crystalline silver and are in good agreement with the standard JCPDS card No. 04-0783. The d-spacing values (2.36-1.18 Å), as reported for standard Ag, are also in line with the values observed. The presence of characteristic FCC reflections provides good evidence for the generation of crystalline silver nanoparticles. The strong (111) diffraction peak indicates a preferred orientation, which is a common property of AgNPs. The moderate FWHM broadening and crystallite size of ~16 nm indicated that soluble starch indeed served as a reducing and capping agent, inhibiting particle growth and preserving the crystal's nanoscale crystallinity. No impurity peaks were observed in metallic silver nanoparticles: phase-pure metallic silver nanoparticles were reported [14][15].

Scanning Electron Microscopy (SEM) analysis

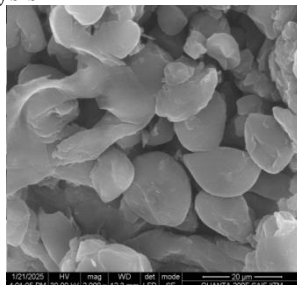


Figure 3. SEM of SS-AgNPs

The surface structure of the synthesized silver nanoparticles were studied using a FEI Quanta FEG 200F scanning electron microscopy technique under a rate of 30 kV. The SEM micrograph (Figure 3) indicates the presence of SS-AgNPs with quasi-spherical with agglomeration. The crystalline pattern, which resembles a sheet, indicates that the biopolymer matrix contains the silver nanoparticles, which tend to agglomerate during sample drying [16]. This kind of aggregation is also common in biopolymer-mediated nanoparticle synthesis, where polymer chains anchor the particles together but also the particles do hold together after solvent is taken away. For this reason, while individual nanoparticles could not be distinctly disentangled due to the nanocomposite structure, the very rough and granular finish on the surface indicates that nanoscale silver particles were embedded in the biopolymer formation. The general morphology indicates good nanoparticle formation, but it also demonstrates the high degree of dependence of agglomeration upon drying and polymer content [17].

Energy Dispersive X-ray Spectroscopy (EDS) Analysis

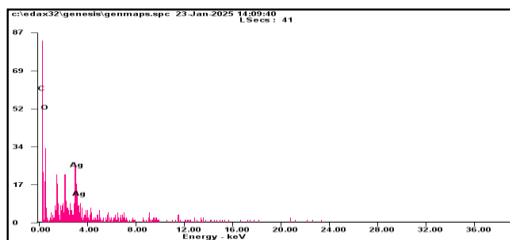


Figure 4. EDS spectrum of SS-AgNPs

Table 2. Elemental composition (Wt% & At%) of SS-AgNPs

Element	Wt%	At%
C	46.31	57.82
O	43.48	40.76
Ag	10.21	01.42

EDS analysis was carried out using an Oxford Instruments INCA system integrated with the SEM. The EDS analysis showed that the composite material is mainly carbon and oxygen, contributing 46.31 wt% (57.82 at%) and 43.48 wt% (40.76 at%), respectively. Soluble starch polymer matrix is the primary surface material. A lower but quite an important amount of silver (10.21 wt%, 1.42 at%) was further detected, indicating the successful addition of Ag in the system. The relatively lower atomic percent of Ag in comparison with carbon and oxygen indicate that the silver nanoparticles are embedded in or coated by the polymer matrix as opposed to being exclusively surface exposed [18].

Transmission Electron Microscopy (TEM) analysis

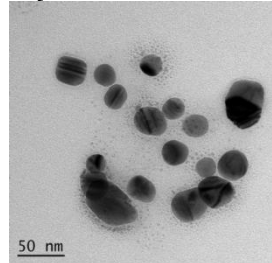


Figure 5. TEM micrograph showing SS-AgNPs

FEI Tecnai G2 Spirit Bio-Twin TEM was used to examine the morphology of the synthesized nanoparticles. The particle size was determined using ImageJ software. The TEM image is shown in Figure 5, and the micrograph contains a scale bar of 50 nm. TEM image indicate that the nanoparticles predominantly were spherical, smooth with uniform spacing, with negligible aggregation. The mean particle size was found to be 25.26 nm which is consistent with XRD-derived crystallite size considering particle aggregation. The smaller than average size distribution indicates that soluble starch had a very strong control on nucleation and growth, and produced stable nanoparticles [19][20].

Antioxidant activity

Antioxidant activity is the ability of a chemical or biological system to neutralize free radicals preventing cell membranes from oxidative damage [21]. If harmful free radicals (e.g. reactive oxygen species - ROS) are present, they may lead to lipid peroxidation, DNA damage and protein degradation. Antioxidants function in this way by donating electrons or hydrogen atoms to stabilize those radicals, thereby protecting cells and other forms of material from oxidative stress [22]. The surface reactivity and optical properties of soluble starch silver nanoparticles (AgNPs) would hinder antioxidant assays from functioning well. AgNPs can change the color intensity or absorption of assay reagents like DPPH, ABTS, or FRAP, which can lead to overestimation or underestimation of the real antioxidant capacity. Starch itself is noted for mild reducing properties which may also factor into the assay results. As such, proper controls and blank corrections are essential when evaluating the antioxidant potentials of soluble starch AgNPs [23].

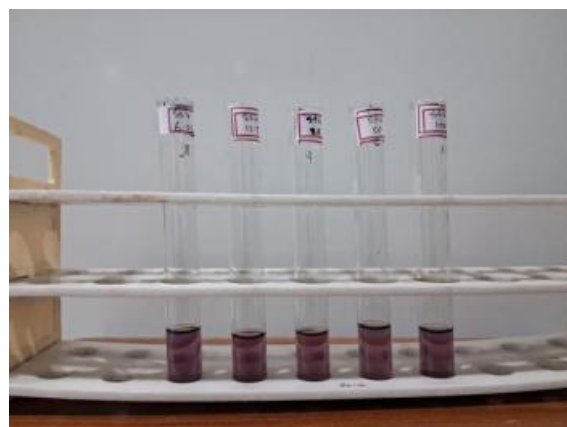


Figure 6. Visual DPPH color change after treatment with SS-AgNPs

Table 3. DPPH radical scavenging activity of soluble starch silver nanoparticles at different concentrations.

Concentration	Absorbance 1	Absorbance 2	% of Inhibition 1	% of Inhibition 2	Mean % of Inhibition
6.25	0.973	0.975	1.017	0.83	0.9235
12.5	0.949	0.951	3.45	3.22	3.335
25	0.882	0.887	10.27	9.76	10.015
50	0.843	0.848	14.24	13.74	13.99
100	0.821	0.824	16.48	16.17	16.325
IC₅₀	303.453196				

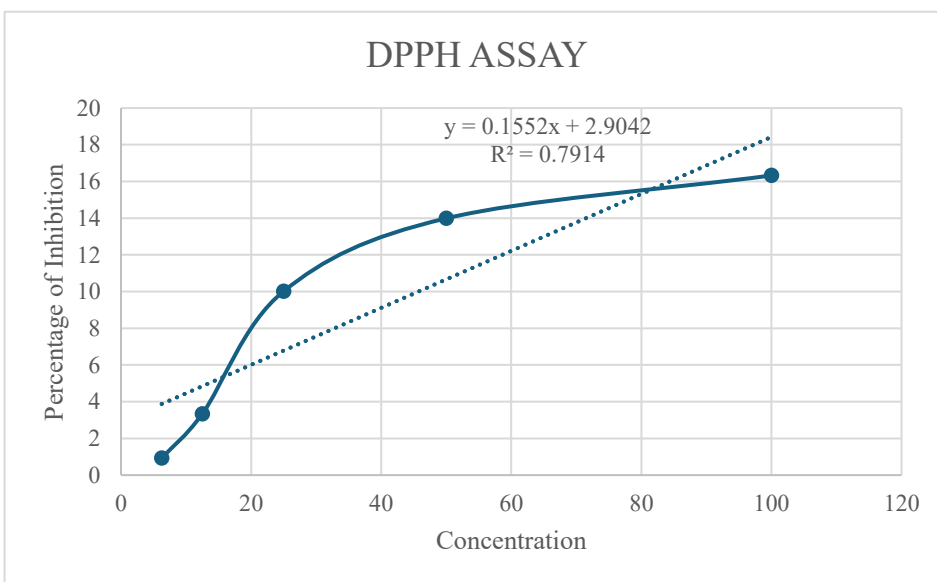


Figure 7. Concentration-dependent DPPH radical scavenging activity of soluble starch silver nanoparticles.

DPPH (1,1-diphenyl-2-picrylhydrazyl) is a stable free radical, which appears to be deep violet in methanol having an absorption of 520 nm. With the reduction of DPPH in the presence of an antioxidant a color change from deep violet to pale yellow results. A decrease in absorbance directly correlates to the radical scavenging capacity of the sample. A DPPH stock solution was prepared in methanol. The stock solution was then diluted with methanol to obtain a working solution having an absorbance of 0.98 ± 0.02 at 520 nm. 1 mg soluble starch silver nanoparticles was dispersed in 1 mL distilled water. To attain concentrations of 6.25, 12.5, 25, 50, and 100 μ g/mL, they were serially diluted. The ascorbic acid was dissolved in distilled water (1 mg/mL) and diluted to the original concentrations.

Pipette 2 mL (for control, the standard or sample) of the DPPH working solution into each test tube. Add 100 μ L to tubes (in which each concentration of the SS-AgNPs sample is contained). Separate standard tubes by adding 100 μ L of each concentration of ascorbic acid. The tubes must be all kept at room temperature in the dark for 30 minutes to promote

reaction. Using the UV-Visible spectrophotometer, check absorbance at 520 nm., with methanol used as a blank. Calculated the % inhibition of each concentration with the formula,

$$\% \text{ of inhibition} = \frac{\text{OD of control} - \text{OD of sample}}{\text{OD of control}} \times 100$$

Soluble starch silver nanoparticles exhibited a unique concentration-dependent scavenging action on DPPH radicals. For the low concentrations tested (6.25 µg/mL), the response was minimal (0.92 %), while at the high concentration (100 µg/mL), it attained 16.32 % inhibition. The IC₅₀ value obtained for these nanoparticles was 303.45 µg/mL, revealing relatively weak antioxidant activity. In comparison, ascorbic acid showed much enhanced scavenging activity at all concentrations, usually >80% inhibition at 100 µg/mL with IC₅₀ at 6 - 10 µg/mL. This observation highlights the more effective radical scavenging capacity of ascorbic acid as a standard antioxidant, albeit in comparison to starch-based silver NPs with moderate antioxidant activity. Nanoparticles are highly active due to the presence of starch (capping and stabilizing agent), thus contributing to the antioxidant activity. This compound has hydroxyl groups that can donate electrons or hydrogen atoms to quench the free radicals. Silver does not by itself scavenge radicals, but interaction with polysaccharides can influence surface chemistry and, in extension, electron transfer. Altered performance of silver compounds has also been observed in those polysaccharide-dependent AgNPs where the capping agent significantly enhances antioxidant effect.

Studies showed that AgNPs prepared from polysaccharides had more effective DPPH scavenging against their precursor extracts with inhibition of 10-30% in the presence of polysaccharides (~40 µg/mL), and >90% in the presence of hydrochloric acid and hydroxyl groups, at a concentration of 100 µg/mL [24]. Optimization of synthesis conditions has been shown to greatly improve radical scavenging efficiency. The value obtained, IC₅₀ of starch-based AgNPs, is relatively high, meaning they do not have the efficiency of small molecule antioxidants like ascorbic acid, but can be important in cases in which a moderate, sustained antioxidant activity is required. For instance, in the fields of biomedicine and food packaging, these nanoparticles providing a gradual radical scavenging behaviour are applicable and have properties that promote the reduction of oxidative stress without inducing abrupt changes in redox imbalance.

Cell viability and proliferation-based wound healing potential of Soluble Starch-Mediated Silver Nanoparticles

Wound healing is a complex, dynamic and intricate biological process aimed at restoring tissue integrity following injury. The process includes several overlapping phases (hemostasis, inflammation, proliferation and remodeling) [25]. It is notable that keratinocyte migration and proliferation, particularly in the proliferative phase, contribute to promoting both re-epithelialization and the reestablishment of epidermal continuity. The HaCaT human keratinocyte cell line is known to be an ideal in vitro model for skin regeneration studies and investigating mechanistic processes involved in wound healing [26]. Several recent advances in nanotechnology have shown promise behind the use of silver nanoparticles (AgNPs) for wound care owing to their strong antimicrobial and antioxidant capabilities. However, the cytotoxicity of chemically synthesized AgNPs often curtails their use in biomedicine. Green synthesis techniques based on natural polymers are biocompatible and eco-friendly substitutes. Soluble starch, a natural polysaccharide, has been extensively studied for its efficiency as both reducing and stabilizing agent in the synthesis of silver nanoparticles, to improve stability as well as reduce toxicity [27]. SS-AgNPs were evaluated in HaCaT cells for their cytotoxicity and wound healing effect by employing the MTT assay for the study. The detection of SS-AgNPs was found to have a non-cytotoxic profile and augmented proliferation indicating SS-AgNPs as potential candidates for therapeutic application for wound healing [28]. HaCaT cells (NCCS, Pune) were grown in Dulbecco's Modified Eagle Medium (DMEM) supplemented with 10% Fetal Bovine Serum (FBS) and 1% Penicillin-Streptomycin. Cells were kept at 37 °C in a 5% CO₂ humidified incubator. For the cytotoxicity analysis, 10,000 cells/well plated on a 96-well plate were incubated for 24 h to allow cell attachment. The cells were exposed to various concentrations of SS-AgNPs (1, 10, 50, 100, 250, 500, and 1000 µM) prepared in serum-free DMEM. Untreated cells and blanks without MTT were included in the control groups. To each well, 20 µL of MTT (5 mg/mL) was added after 24 h treatment and incubated for 2 h; the formazan crystals were dissolved in 100 µL DMSO, and absorbance was determined at 540 nm by ELISA reader (Bio-Rad iMark, USA).

Table 4. IC₅₀ value of SS-AgNPs in HaCaT cells determined by MTT assay.

Sample code	IC ₅₀ value (µM) Mean ± SEM
SS-AgNPs	Not converged

Table 5. Replicate absorbance values used for cell viability calculation.

	Final Replicate Values

Sample Conc.	1	2	3	4
0	108.0357143	97.32142857	99.10714286	95.53571429
1	126.7857143	123.2142857	108.9285714	108.9285714
10	139.2857143	148.2142857	132.1428571	130.3571429
50	170.5357143	158.0357143	141.9642857	140.1785714
100	173.2142857	183.9285714	175	173.2142857
250	193.75	186.6071429	186.6071429	181.25
500	163.3928571	170.5357143	159.8214286	163.3928571
1000	156.25	150.8928571	134.8214286	133.0357143

Table 6. Cell viability (%) of HaCaT cells treated with SS-AgNPs at different concentrations.

Sample Conc.	Mean	Standard Deviation	Standard Error of Mean	Number of Test Replicates
0	100	5.552011341	2.776005671	4
1	116.9642857	9.392698713	4.696349357	4
10	137.5	8.117965296	4.058982648	4
50	152.6785714	14.35992629	7.179963144	4
100	176.3392857	5.129073792	2.564536896	4
250	187.0535714	5.129073792	2.564536896	4
500	164.2857143	4.493949069	2.246974534	4
1000	143.75	11.57275125	5.786375624	4

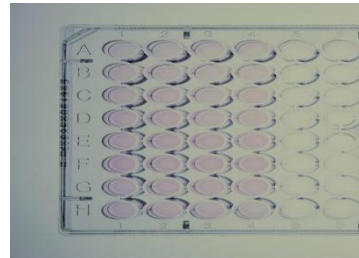


Figure 8. Representative layout of a 96-well plate used in the MTT cytotoxicity assay.

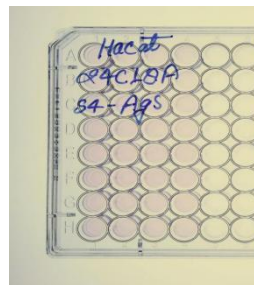


Figure 9. Morphological appearance of HaCaT cells after treatment with SS-AgNPs.

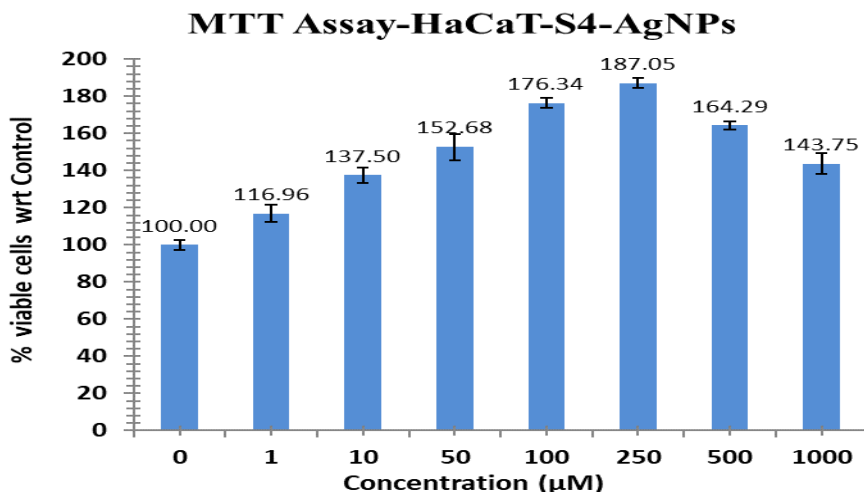


Figure 10. MTT assay showing the effect of SS-AgNPs on HaCaT cell viability

% Cell viability is calculated using below formula:

$$\text{Cell viability (\%)} = \frac{\text{Mean absorbance of treated cells}}{\text{Mean absorbance of untreated control cells}} \times 100$$

Results were shown by Mean \pm Standard Error of Mean from quadruplicate samples. The IC₅₀ values were calculated by GraphPad Prism 6. Morphological changes were examined under inverted microscope (Olympus EK2) with a digital CMOS camera.

SS-AgNPs produced no cytotoxic effects on HaCaT cells at concentrations as high as 1000 μ M whereas a concentration-dependent improvement in viability was seen, reaching a maximum value of around 187% at 250 μ M as compared to the control. IC₅₀ could not be calculated due to absence of cytotoxicity even at highest tested concentration. The IC₅₀ value could not be determined (non-convergent), which again confirms non-cytotoxicity of the nanoparticles.

The results also suggest that SS-AgNPs are non-toxic to cells and promote proliferation of keratinocytes, important components of the wound healing process. According to this study, the higher cell viability over 100% indicates a positive effect on cellular metabolism and proliferation, potentially advancing the healing process of wounds. Starch-stabilized AgNPs, on the other hand, are more biocompatible than AgNPs synthesized through harsh reducing agents due to their natural polysaccharide coating. The reported proliferative response is in line with previous studies demonstrating that polysaccharide-mediated nanoparticles favor keratinocyte growth and adhesion. The antimicrobial and antioxidant properties of AgNPs provide added benefits in wound healing by preventing microorganism infection, as well as by relieving oxidative stress. Thus the synergistic safety, bioactivity, and proliferation features of soluble starch-stabilized AgNPs combined point to the applicability of soluble starch-stabilized AgNPs as potential components in wound-healing materials such as gels, creams and dressings.

With this result, soluble starch-mediated silver nanoparticles (SS-AgNPs) exhibited superior biocompatibility and stimulated HaCaT keratinocyte proliferation and lacked cytotoxic effect which is observed in some of the cells. The results indicate their promising roles as safe and efficient agents in wound healing. Their therapeutic efficacy should be validated in clinical wound management using additional *in vivo* studies.

Anticancer activity

In this study soluble starch mediated silver nanoparticles (SS-AgNPs) were evaluated for their anticancer potential against the MCF-7 human breast adenocarcinoma cell line. The MTT assay was used, a reliable colorimetric technique for deciding cell viability and cytotoxicity [29].

Silver nanoparticles AgNPs play a unique role in cancer treatment with its biological and chemical properties. Silver nanoparticles are reported to exhibit selective cytotoxicity and induce oxidative stress, leading to cell death or inhibition of tumor growth [30][31].

MTT assay is a colorimetric assay used for the determination of cell proliferation and cytotoxicity, based on reduction of the yellow coloured water soluble tetrazolium dye MTT to formazan crystals [32]. Mitochondrial lactate dehydrogenase produced by live cells reduces MTT to insoluble formazan crystals, which upon dissolution into an appropriate solvent exhibits purple colour, the intensity of which is proportional to the number of viable cells and can be measured spectrophotometrically at 570nm [33].

Cell line: MCF7-Human breast adenocarcinoma cell lines (NCCS, Pune), Cell culture medium: DMEM with high Glucose - (#11965-084, Gibco, Invitrogen), Fetal Bovine Serum (#RM10432, Himedia), MTT Reagent (# 4060 Himedia), DMSO (#PHR1309, Sigma), D-PBS (#TL1006, Himedia), Doxorubicin (Cat No: D1515, Sigma) 96-well plate for culturing the cells (130188, Biolite, Thermo), T25 flask (# 12556009, Biolite – Thermo), 50 ml centrifuge tubes (# 546043 TARSONS), 1.5 mL centrifuge tubes (TARSONS), 10 mL serological pipettes (TARSONS), 10 to 1000µL tips (TARSONS)

Equipment: centrifuge (Remi: R-8C), Pipettes: 2-10µL, 10-100µL, and 100-1000µL. Inverted binocular biological microscope (CKX-415F, Olympus, Japan), Biosafety hood (Biobase, China), 37°C incubator with humidified atmosphere of 5% CO₂ (Healforce, China), 96well plate reader (ELX-800, BioTek, CA, USA).

Assay controls

- (i) Medium control (medium without cells)
- (ii) Negative control (medium with cells but without the experimental drug/compound)
- (iii) Positive control (medium with cells treated by 1ug/ml of Doxorubicin)
- (iv) Extracellular reducing components such as ascorbic acid, cholesterol, alpha-tocopherol, dithiothreitol present in the culture media may reduce the MTT to formazan. To account for this reduction, it is important to use the same medium in control as well as test wells.

Maintenance of cell line

The MCF7 (Human breast adenocarcinoma cell line) was purchased from NCCS, Pune, India. The cells were maintained in DMEM with high glucose media supplemented with 10 % FBS along with the 1% antibiotic-antimycotic solution in the atmosphere of 5% CO₂, 18-20% O₂ at 37 °C temperature in the CO₂ incubator and sub-cultured for every 2 days. Passage number of MCF7 cells was 75 used in present study. Seed 200µL cell suspension in a 96-well plate at required cell density (20,000 cells per well), without the test agent. Allow the cells to grow for about 24 h. Add appropriate concentrations of the given test agents diluted in complete media. Incubate the plate for 24hrs at 37°C in a 5% CO₂ atmosphere. After the incubation period, takeout the plates from incubator, and remove spent media and add MTT reagent to a final concentration of 0.5mg/mL of total volume. Wrap the plate with aluminium foil to avoid exposure to light. Return the plates to the incubator and incubate for 3 hours. Within one experiment, incubation time should be kept constant while making comparisons. Remove the MTT reagent and then add 100µL of solubilisation solution (DMSO). Gentle stirring in a gyratory shaker will enhance dissolution. Occasionally, pipetting up and down may be required to completely dissolve the MTT formazan crystals especially in dense cultures. Read the absorbance on a spectrophotometer or an ELISA reader at 570nm wavelength. Cell viability (%) was calculated using the formula:

$$\% \text{ cell viability} = \frac{\text{Mean absorbance of treated cells}}{\text{Mean absorbance of untreated control cells}} \times 100$$

The IC₅₀ value was calculated from the dose-response curve using linear regression equation i.e. $y=mx+c$
 $Y = 50$, M and C values were derived from the viability graph.

Drug concentration details

In this study, given test compounds were evaluated to analyze the cytotoxicity effect on MCF7 cells. The concentrations of the test compounds used to treat the cells as follows:

Table 7. The concentrations of the test compounds used to treat the cells

Sl.No	Culture condition	Cell lines	Concentration applied to cells
1.	Untreated	MCF7	No treatment
2.	Blank	-	Only media without cells
3.	Std control (Dox)	MCF7	1ug/ml
4.	Test compounds	MCF7	5 (6.25, 12.5, 25, 50, 100 µg/mL)

By using the MTT assay, the cytotoxic potential of soluble starch stabilized silver nanoparticles (SS-AgNPs) was assessed on MCF-7 human breast adenocarcinoma cells. With increasing nanoparticle concentration, the percentage of viable cells decreased progressively. It indicates a strong dose dependent cytotoxic effect. Cell viability at the lowest concentration [6.25µg/mL], was 68.80%. Then declined to 55.37% at 12.5µg/mL and 38.505 at 25µg/mL. At higher concentrations a pronounced reduction was observed. Only 21.27% at 50µg/mL and 0.69% at 100µg/ml compared to 100% viability in untreated control cells 52.83% viability is exhibited by the standard drug Doxorubicin (1µg/mL).

Table 8. MTT assay showing absorbance, cell viability (%) and IC₅₀ values of SS-AgNPs

Concentration Unit: µg/mL		Incubation:24hrs			Cell line: MCF7			PN-75
Parameter	Blank	Untreated	Dox-1µg	6.25	12.5	25	50	100
Abs reading 1	0.086	2.533	1.343	1.816	1.482	1.015	0.607	0.107
Abs reading 2	0.084	2.596	1.447	1.766	1.434	1.064	0.618	0.097
Mean abs	0.085	2.5645	1.395	1.791	1.458	1.0395	0.6125	0.102
Mean abs (Sample-Blank)		2.4795	1.31	1.706	1.373	0.9545	0.5275	0.017
STANDARD DEVIATION		0.044547727	0.073539105	0.035355339	0.033941125	0.034648232	0.007778175	0.007071068
STANDARD ERROR		0.0315	0.052	0.025	0.024	0.0245	0.0055	0.005
Cell Viability %		100	52.83323251	68.80419439	55.37406735	38.49566445	21.27445049	0.685622101
IC₅₀ value	14.69µg/mL							

Table 9. Dose dependent cell viability of MCF-7 cells treated with SS-AgNPs and corresponding IC₅₀ value

MTT assay SS-AgNPs vs MCF7 (% cell viability)	
Culture condition	% cell viability
Untreated	100.00
Dox-1µg	52.83
SS-6.25µg	68.80
SS-12.5µg	55.37
SS-25µg	38.50
SS-50µg	21.27
SS-100µg	0.69
IC₅₀ conc (µg/mL)	14.69µg/mL

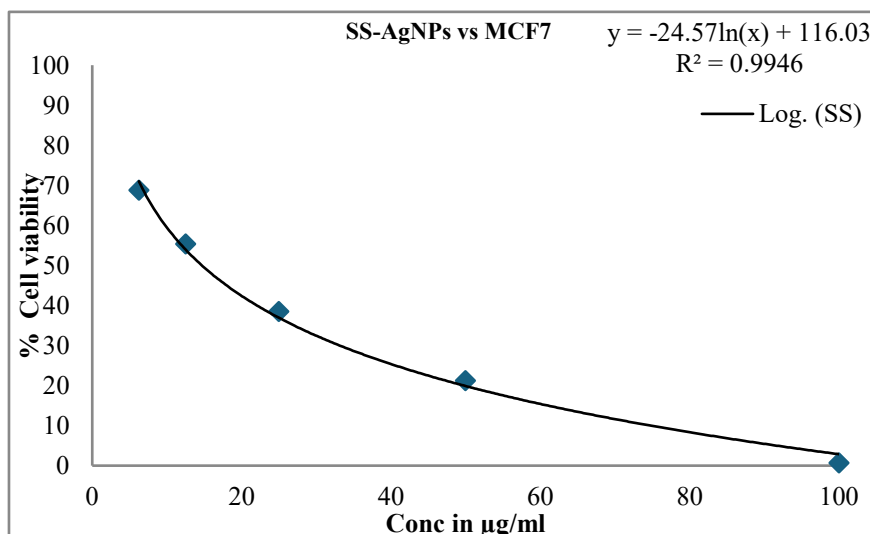


Figure 11. Dose-response curve showing the reduction in MCF-7 cell viability with increasing concentrations of SS-AgNPs.

The calculated IC₅₀ value for SS-AgNPs against MCF-7 cells was 14.69µg/ml in the viability curve. It demonstrated significant antiproliferative efficiency. Under an inverted microscope Morphological observations revealed distinct cellular shrinkage and loss of adherence in treated wells. It was consistent with apoptotic changes induced by cytotoxic

stress. The treatment with SS-AgNPs revealed a clear dose dependent reduction in MCF-7 Cell viability. The Untreated control exhibited 100% viability. The standard drug Doxorubicin (1 μ g/mL) reduced viability to 53.83%. On the other hand, SS-AgNPs significantly decreased cell viability as concentration increased.

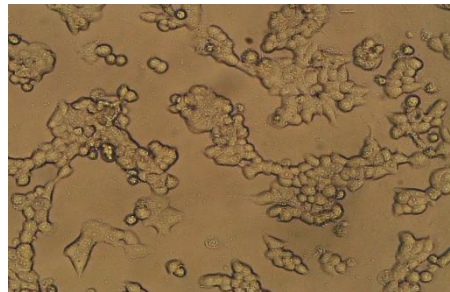


Figure 12a. Control – Cells are healthy, normal morphology and membrane structure intact

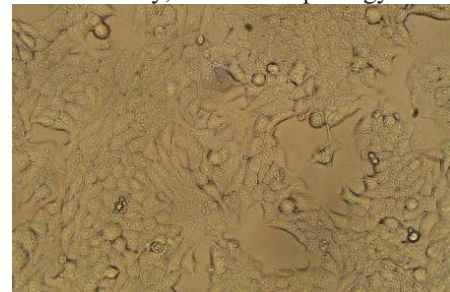


Figure 12b. Untreated – Absence of visible morphologic changes, dense layer of healthy cells

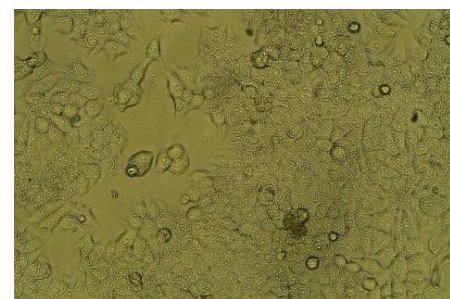


Figure 12c. 6.25 μ g/mL – Small cell density drop with early rounding

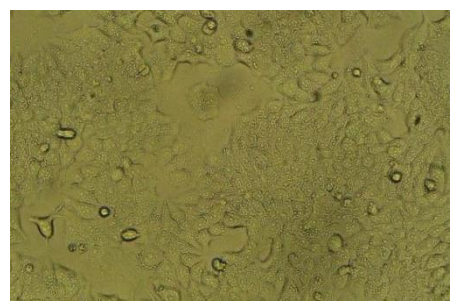


Figure 12d. 12.5 μ g/mL – Cell rounding and decrease in number of viable cells

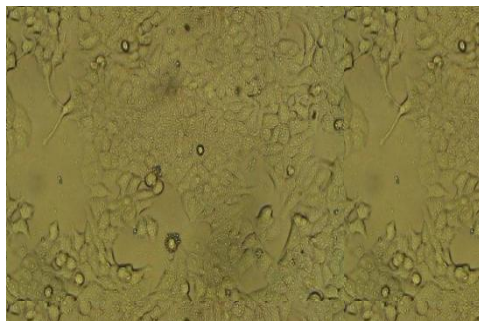


Figure 12e. 25 µg/mL – Cells shrink and detach from the surface

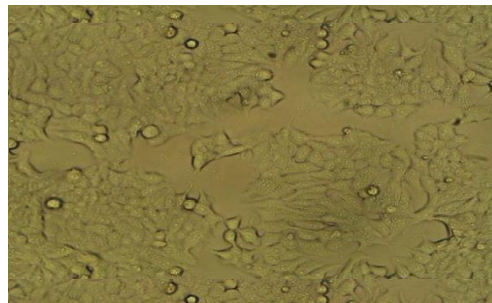


Figure 12f. 50 µg/mL – Marked cytotoxicity with considerable cell integrity loss



Figure 12g. 100 µg/mL – Acute cell damage with ample membrane disruption and very low cell survival

Conclusion

The SS-AgNPs were synthesized using green method. The structural characterization showed that the nanoparticles were highly crystalline and predominantly spherical with an average crystallite size of approximately 15.83 nm and average particle size of around 25 nm. The soluble starch proved to be the reducing and stabilizing material, as confirmed by SEM, EDS and TEM measurements to ensure uniform nucleation, controlled particle growth and successful incorporation of silver into the starch matrix. No impurities were observed, which suggested the purity and stability of the synthesized nanoparticles.

It was subsequently found that SS-AgNPs showed moderate antioxidant activity in the biological experiments by DPPH IC_{50} 303.45 µg/mL, which demonstrated that the radical scavenging activity was both slow and lasting because of the role of the polysaccharide capping layer. The nanoparticles displayed no toxicity to normal HaCaT keratinocytes. They promoted cell proliferation significantly at optimized concentrations to reach around 187% viability. This behavior explains their great potential for wound healing with keratinocyte proliferation having crucial significance in the process of re-epithelialization and tissue regeneration. SS-AgNPs, in contrast, demonstrated higher anti-cancer activity towards MCF-7 human breast cancer cells with a relatively low IC_{50} value of 14.69 µg/mL. These unequivocal dose-dependent and cytotoxic actions were reflected by dose-dependent decline in cell viability, and morphologically pronounced apoptosis as expected.

Overall, these results indicate such high-biocompatibility dualities as these nanoparticles--proliferative to normal and cytotoxic to cancer--and thus point towards a prospective selective therapy. Further experiments are warranted to investigate the therapeutic application of SS-AgNPs outside the *in vitro*. *In vivo* wound healing should be measured, including *in vivo* studies on wound repair, cellular uptake by ROS-dependent cytotoxicity and also full toxic profile,

including hemocompatibility, and genotoxicity. The formulation of SS-AgNPs in the form of gels, films, creams, dressings, antimicrobial coatings and cosmetics may expand their application in practical sectors. The stability and biodegradability, biocompatibility provide further indications for usage in food packaging, agricultural and environmental remediation. All these work together establish the soluble starch-based silver nanoparticles as a safe, eco-friendly and multifunctional nanomaterial with high potential for biomedical use, in particular wound healing and cancer treatment.

Author contributions

Oshin M Manchu carried out the experiments, collected and analyzed the data, and wrote the original draft of the manuscript. Dr. S. Jasmin Sugantha Malar supervised the research work and provided overall guidance.

Funding

The authors did not receive any financial support from any organization for this work.

Acknowledgement

The authors sincerely thank Manonmaniam Sundaranar University, Abishekappatti, Tirunelveli - 627012, Tamil Nadu for academic support. The authors also thank the Women's Christian College, Nagercoil-629001, for providing the necessary laboratory facilities to carry out this research work.

REFERENCES

1. Kvítek, O., Siegel, J., Hnatowicz, V. and Švorčík, V., 2013. Noble metal nanostructures influence of structure and environment on their optical properties. *Journal of Nanomaterials*, 2013(1), p.743684.
2. Baker, C., Pradhan, A., Pakstis, L., Pochan, D.J. and Shah, S.I., 2005. Synthesis and antibacterial properties of silver nanoparticles. *Journal of nanoscience and nanotechnology*, 5(2), pp.244-249.
3. Burduşel, A.C., Gherasim, O., Grumezescu, A.M., Mogoantă, L., Ficai, A. and Andronescu, E., 2018. Biomedical applications of silver nanoparticles: an up-to-date overview. *Nanomaterials*, 8(9), p.681.
4. Saravanakumar, K., Sriram, B., Sathyaseelan, A., Mariadoss, A.V.A., Hu, X., Han, K.S., Vishnupriya, V., MubarakAli, D. and Wang, M.H., 2021. Synthesis, characterization, and cytotoxicity of starch-encapsulated biogenic silver nanoparticle and its improved anti-bacterial activity. *International Journal of Biological Macromolecules*, 182, pp.1409-1418.
5. Gamage, A., Thiviy, P., Mani, S., Ponnusamy, P.G., Manamperi, A., Evon, P., Merah, O. and Madhujith, T., 2022. Environmental properties and applications of biodegradable starch-based nanocomposites. *Polymers*, 14(21), p.4578.
6. Morán, D., López-Carballo, G., Gavara, R., Gutiérrez, G. and Matos, M., 2025. Starch-silver hybrid nanoparticles: A novel antimicrobial agent. *Colloids and Surfaces A: Physicochemical and Engineering Aspects*, 717, p.136797.
7. Bedlovičová, Z., Strapáč, I., Baláž, M. and Salayová, A., 2020. A brief overview on antioxidant activity determination of silver nanoparticles. *Molecules*, 25(14), p.3191.
8. Buttacavoli, M., Albanese, N.N., Di Cara, G., Alduina, R., Falieri, C., Gallo, M., Pizzolanti, G., Gallo, G., Feo, S., Baldi, F. and Cancemi, P., 2017. Anticancer activity of biogenerated silver nanoparticles: an integrated proteomic investigation. *Oncotarget*, 9(11), p.9685.
9. Lin, J., Huang, Z., Wu, H., Zhou, W., Jin, P., Wei, P., Zhang, Y., Zheng, F., Zhang, J., Xu, J. and Hu, Y., 2014. Inhibition of autophagy enhances the anticancer activity of silver nanoparticles. *Autophagy*, 10(11), pp.2006-2020.
10. Kaler, A., Mittal, A.K., Katariya, M., Harde, H., Agrawal, A.K., Jain, S. and Banerjee, U.C., 2014. An investigation of in vivo wound healing activity of biologically synthesized silver nanoparticles. *Journal of nanoparticle research*, 16(9), p.2605.
11. Maghima, M. and Alharbi, S.A., 2020. Green synthesis of silver nanoparticles from Curcuma longa L. and coating on the cotton fabrics for antimicrobial applications and wound healing activity. *Journal of Photochemistry and Photobiology B: Biology*, 204, p.111806.
12. Kelly, K.L., Coronado, E., Zhao, L.L. and Schatz, G.C., 2003. The optical properties of metal nanoparticles: the influence of size, shape, and dielectric environment. *The Journal of Physical Chemistry B*, 107(3), pp.668-677.
13. Chevron, P., Gouanvéd, F. and Espuche, E., 2014. Green synthesis of colloid silver nanoparticles and resulting biodegradable starch/silver nanocomposites. *Carbohydrate polymers*, 108, pp.291-298.
14. Mehta, B.K., Chhajlani, M. and Shrivastava, B.D., 2017, April. Green synthesis of silver nanoparticles and their characterization by XRD. In *Journal of physics: conference series* (Vol. 836, No. 1, p. 012050). IOP Publishing.
15. Bykkam, S., Ahmadipour, M., Narisngam, S., Kalagadda, V.R. and Chidurala, S.C., 2015. Extensive studies on X-ray diffraction of green synthesized silver nanoparticles. *Adv. Nanopart*, 4(1), pp.1-10.
16. Ayala Valencia, G., Cristina de Oliveira Vercik, L., Ferrari, R. and Vercik, A., 2013. Synthesis and characterization of silver nanoparticles using water-soluble starch and its antibacterial activity on *Staphylococcus aureus*. *Starch-Stärke*, 65(11-12), pp.931-937.

17. Pascu, B., Negrea, A., Ciopec, M., Duteanu, N., Negrea, P., Nemeş, N.S., Seiman, C., Marian, E. and Micle, O., 2021. A green, simple and facile way to synthesize silver nanoparticles using soluble starch. pH studies and antimicrobial applications. *Materials*, 14(16), p.4765.
18. Abdelsalam, Nader R., Moustafa MG Fouda, Ahmed Abdel-Megeed, Jamaan Ajarem, Ahmed A. Allam, and Mehrez E. El-Naggar. "Assessment of silver nanoparticles decorated starch and commercial zinc nanoparticles with respect to their genotoxicity on onion." *International journal of biological macromolecules* 133 (2019): 1008-1018.
19. Hebeish, A., Shaheen, T.I. and El-Naggar, M.E., 2016. Solid state synthesis of starch-capped silver nanoparticles. *International journal of biological macromolecules*, 87, pp.70-76.
20. Khan, Z., Singh, T., Hussain, J.I., Obaid, A.Y., Al-Thabaiti, S.A. and El-Mossalamy, E.H., 2013. Starch-directed green synthesis, characterization and morphology of silver nanoparticles. *Colloids and Surfaces B: Biointerfaces*, 102, pp.578-584.
21. Varadharaj, V., Ramaswamy, A., Sakthivel, R., Subbaiya, R., Barabadi, H., Chandrasekaran, M. and Saravanan, M., 2020. Antidiabetic and antioxidant activity of green synthesized starch nanoparticles: an in vitro study. *Journal of Cluster Science*, 31(6), pp.1257-1266.
22. Sreelekha, E., George, B., Shyam, A., Sajina, N. and Mathew, B., 2021. A comparative study on the synthesis, characterization, and antioxidant activity of green and chemically synthesized silver nanoparticles. *BioNanoScience*, 11(2), pp.489-496.
23. Keshari, A.K., Srivastava, R., Singh, P., Yadav, V.B. and Nath, G., 2020. Antioxidant and antibacterial activity of silver nanoparticles synthesized by Cestrum nocturnum. *Journal of Ayurveda and integrative medicine*, 11(1), pp.37-44.
24. Yousaf, H., Mehmood, A., Ahmad, K.S. and Raffi, M., 2020. Green synthesis of silver nanoparticles and their applications as an alternative antibacterial and antioxidant agents. *Materials Science and Engineering: C*, 112, p.110901.
25. Muneeswaran, T., Maruthupandy, M., Mary, A.S., Vennila, T., Rajaram, K., Ramakritinan, C.M. and Quero, F., 2023. Starch-mediated synthesis of chitosan/silver nanocomposites for antibacterial, antibiofilm and wound healing applications. *Journal of Drug Delivery Science and Technology*, 84, p.104424.
26. Aktürk, A., Taygun, M.E., Güler, F.K., Goller, G. and Küçükbayrak, S., 2019. Fabrication of antibacterial polyvinylalcohol nanocomposite mats with soluble starch coated silver nanoparticles. *Colloids and Surfaces A: Physicochemical and Engineering Aspects*, 562, pp.255-262.
27. El-Hefnawy, M.E., Alhayyani, S., El-Sherbiny, M.M., Sakran, M.I. and El-Newehy, M.H., 2022. Fabrication of nanofibers based on hydroxypropyl starch/polyurethane loaded with the biosynthesized silver nanoparticles for the treatment of pathogenic microbes in wounds. *Polymers*, 14(2), p.318.
28. Mohanty, S., Mishra, S., Jena, P., Jacob, B., Sarkar, B. and Sonawane, A., 2012. An investigation on the antibacterial, cytotoxic, and antibiofilm efficacy of starch-stabilized silver nanoparticles. *Nanomedicine: Nanotechnology, Biology and Medicine*, 8(6), pp.916-924.
29. Gomathi, A.C., Rajarathinam, S.X., Sadiq, A.M. and Rajeshkumar, S., 2020. Anticancer activity of silver nanoparticles synthesized using aqueous fruit shell extract of Tamarindus indica on MCF-7 human breast cancer cell line. *Journal of drug delivery science and technology*, 55, p.101376.
30. Venugopal, K., Rather, H.A., Rajagopal, K., Shanthi, M.P., Sheriff, K., Illiyas, M., Rather, R.A., Manikandan, E., Uvarajan, S., Bhaskar, M. and Maaza, M., 2017. Synthesis of silver nanoparticles (Ag NPs) for anticancer activities (MCF 7 breast and A549 lung cell lines) of the crude extract of Syzygium aromaticum. *Journal of Photochemistry and Photobiology B: Biology*, 167, pp.282-289.
31. Ramdath, S., Mellem, J. and Mbatha, L.S., 2021. Anticancer and antimicrobial activity evaluation of cowpea-porous-starch-formulated silver nanoparticles. *Journal of Nanotechnology*, 2021(1), p.5525690.
32. Lomelí-Marroquín, D., Medina Cruz, D., Nieto-Argüello, A., Vernet Crua, A., Chen, J., Torres-Castro, A., Webster, T.J. and Cholula-Díaz, J.L., 2019. Starch-mediated synthesis of mono-and bimetallic silver/gold nanoparticles as antimicrobial and anticancer agents. *International journal of nanomedicine*, pp.2171-2190.
33. Hasanin, M., Al Abboud, M.A., Alawlaqi, M.M., Abdelghany, T.M. and Hashem, A.H., 2022. Ecofriendly synthesis of biosynthesized copper nanoparticles with starch-based nanocomposite: antimicrobial, antioxidant, and anticancer activities. *Biological Trace Element Research*, 200(5), pp.2099-2112.

